Brief Communication

Soot Volume Fraction Maps for Normal and Reduced Gravity Laminar Acetylene Jet Diffusion Flames

PAUL S. GREENBERG*
MS 110-3, NASA Lewis Research Center, 21000 Brookpark Road, Cleveland, OH 44135

and

JERRY C. KU
Mechanical Engineering Department, Wayne State University, 5050 Anthony Wayne Drive, Detroit, MI 48202

INTRODUCTION

The study of soot particulate distribution inside gas jet diffusion flames is important to the understanding of fundamental soot particle and thermal radiative transport processes, as well as providing findings relevant to spacecraft fire safety, soot emissions, and radiant heat loads for combustors used in air-breathing propulsion systems. Compared to those under normal gravity (1-g) conditions, the elimination of buoyancy-induced flows is expected to significantly change the flow field in microgravity (0 g) flames, resulting in taller and wider flames with longer particle residence times. Work by Bahadori and Edelman [1] demonstrate many previously unreported qualitative and semi-quantitative results, including flame shape and radiation, for sooting laminar gas jet diffusion flames. Work by Ku et al. [2, 3] report soot aggregate size and morphology analyses, and data and model predictions of soot volume fraction maps [4] for various gas jet diffusion flames. In this study, we present the first 1-g and 0-g comparisons of soot volume fraction maps for laminar acetylene and nitrogen-diluted acetylene jet diffusion flames.

Volume fraction is one of the most useful properties in the study of sooting diffusion flames. The amount of radiation heat transfer depends directly on the volume fraction [4], and this parameter can be measured from line-of-sight extinction measurements. Although most soot aggregates are submicron in size, the primary particles (20 to 50 nm in diameter) are in the Rayleigh limit, so the extinction ($\cong$ absorption) cross section of aggregates can be accurately approximated [5–7] by the Rayleigh solution as a function of incident wavelength, particles' complex refractive index, and particles' volume fraction.

MEASUREMENT AND DATA INVERSION PROCEDURES

Reduced gravity experiments have been conducted using the NASA Lewis Research Center's 2.2-s drop tower facility. The imaging absorption technique [8] developed by the authors is applied to measure full-field flame transmittance over a 50-mm-diameter field of view. The method utilizes solid-state detector arrays coupled with collection optics configured to provide depth-invariant magnification and characterized angular collection efficiency. The beam from a 1.5-mW visible (632.8 nm) laser diode is spatially filtered, expanded, and collimated before passing through the flame. Bandpass and neutral density filters are used to block flame emissions and to optimize the dynamic range of the detected signal. Undesirable coherent imaging effects and fluctuations in source stability are taken into account to improve measurement sensitivity. A system constructed from inexpensive, commercially available components has been demonstrated to determine fractional absorbance of 4×10^{-3}

*Corresponding author.

COMBUSTION AND FLAME 108: 227–230 (1997)

Published by Elsevier Science Inc.

0010-2180/97/$17.00
PII S0010-2180(96)00205-2

at a full-field acquisition rate of 30 Hz with very good repeatability.

A sequence of image frames is recorded throughout the 2.2-s time span of the drop sequence. This sequence includes an unattenuated reference frame acquired prior to ignition under reduced gravity. The transmittance T at each pixel location is calculated as the ratio of intensity I (with the flame) to I_0 (without), and is related to the local soot volume fraction $f_v(r)$ through

$$\frac{I}{I_0} = \exp\left[\int_{-R}^{+R} \frac{6\pi}{\lambda} \mathrm{Im}\left(\frac{m^2-1}{m^2+2}\right) f_v(r)\, dr\right]. \quad (1)$$

Here, λ is the wavelength and we choose $m = 1.7 - i0.7$ as the complex refractive index of soot. The integration is along chord-like paths through the flame. The measured transmittance map was numerically smoothed using a two-dimensional tensor-product spline scheme [8] to minimize spatial noise due to coherent imaging effects. Tomographic reconstruction [9] was then used to calculate local soot volume fractions, assuming the flame is axisymmetric. We have demonstrated [8] that the numerical smoothing yields almost identical results as those from temporal averaging for slowly varying laminar diffusion flames.

RESULTS AND DISCUSSION

Pure acetylene and 50% nitrogen-diluted (by volume) acetylene were injected at a flow rate of 2.3 cc/s into quiescent atmospheric air from a nozzle with i.d. 1.65 mm. The measured maximum attenuations are 26%, 66%, 74%, and 86% for 1-g 50%, 0-g 50%, 1-g pure, and 0-g pure flames, respectively. Although the last three flames are in the optically thick (and hence multiple scattering) limit where Eq. 1 is inaccurate, we were not able to obtain reliable data from other fuels. With the same setup, both 1-g propane and ethylene yield less than 5% attenuation over most of the flame. Attempts to increase the nozzle diameter were restricted by the amount of bottled fuel, while reducing the fuel flow rate caused a delay in reaching steady-state for 0-g flames.

Figure 1 shows soot volume fraction maps, in combined three-dimensional and contour plots, for these flames. As expected from the elimination of buoyancy-induced flow, 0-g flames are taller and wider than their 1-g counterparts. Note the radial scale for 0-g flames is 1.7 times larger than that for 1-g flames. Small extraneous peaks observed along the flame axis are artifacts resulting from tomographic reconstruction [8]. For the pure acetylene flames, soot particles are released from the flame tip (i.e., smoking) under both 1-g and 0-g. The diluted flames, however, only smoke under 0 g. Soot loading at each flame height is calculated by integrating the local volume fraction over the flame cross section. For 1-g flames, the peak soot loading decreases roughly by a factor of 4 from pure to diluted acetylene, whereas Gulder and Snelling [10] reported a factor of 3.3 for co-flow ethylene flames. The peak soot loading in 0-g is approximately four times that in 1-g for the 50%-acetylene flame, and three times that for the pure acetylene flame. For 50%-acetylene flames, the maximum local soot volume fraction under 0-g is about twice that under 1-g. For pure acetylene flames, both 0-g and 1-g volume fraction maps exhibit similar maximum values.

The increase in soot loading from 1-g to 0-g flames is attributed mainly to the increase in particle residence time and the subsequent change in soot radiative heat transfer. In a simulation for 1 cc/s ethylene and propane flames, the elimination of buoyancy-induced flow causes a decrease in the centerline gas velocity by a factor of 10 from 1-g to 0-g, and an increase in the flame height by a factor of 2, resulting in a 20-fold increase in residence time from 1-g to 0-g. Longer residence times will expectedly promote soot formation, growth, and coagulation, and consequently result in higher local soot volume fractions. A larger flame size and a higher soot loading naturally suggest a higher radiant heat loss from the flame and consequently a cooler flame in 0-g. A cooler flame will exhibit less soot oxidation (i.e., burnout), and thus a slower decrease in soot loading. Results from a sophisticated modeling analysis [4], which includes coupled equations for flame structure, soot formation

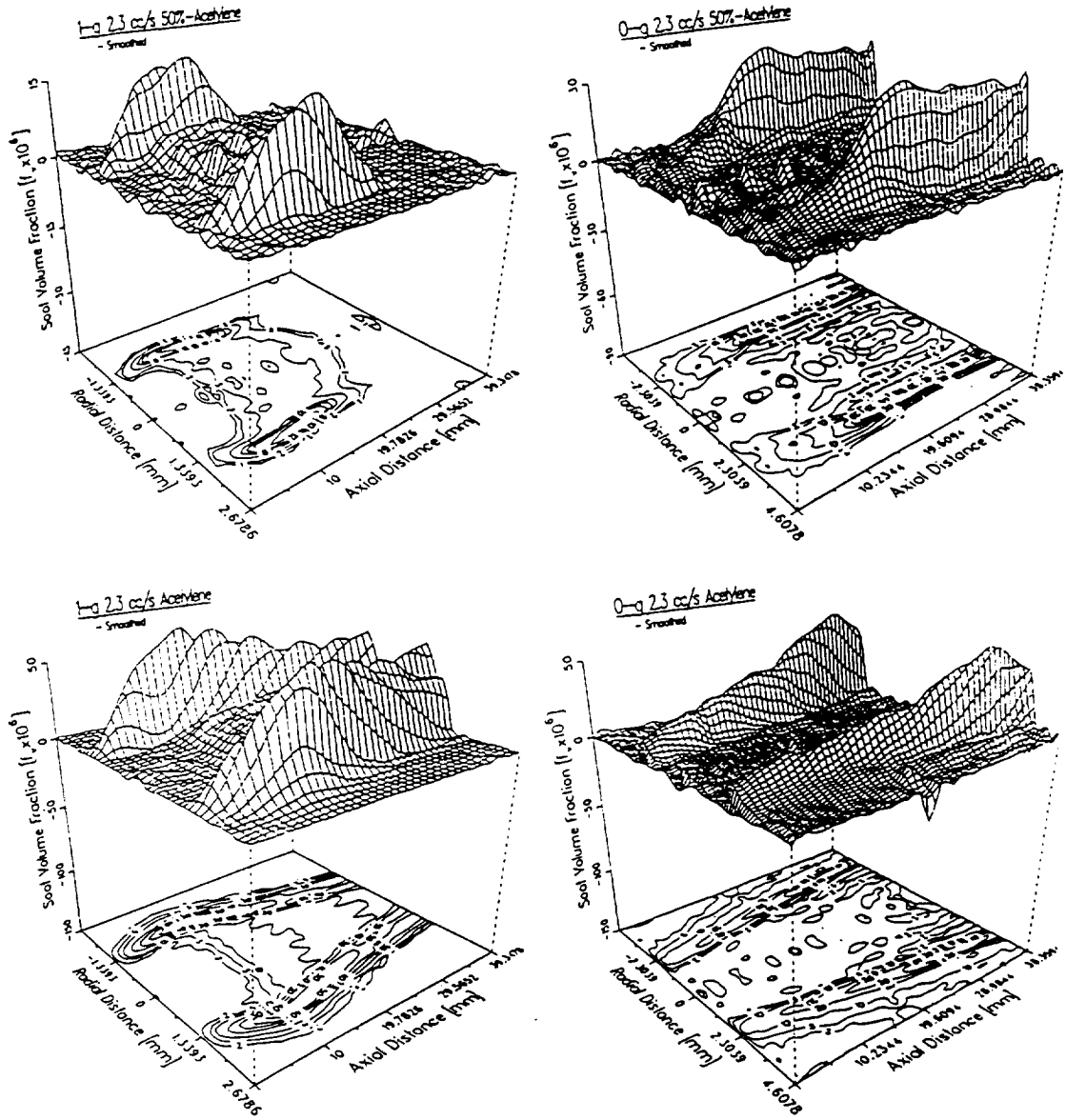

Fig. 1. Combined three-dimensional and contour soot volume fraction distributions for 1-*g* and 0-*g* laminar acetylene and 50%-acetylene jet diffusion flames.

and oxidation, and radiative heat transfer, support the aforementioned conclusions.

J. C. Ku wishes to acknowledge support under NASA grant number NAG3-1265.

REFERENCES

1. Bahadori, M. Y., and Edelman, R. B., *NASA Contractor Report 191109* (1993).
2. Ku, J. C., Griffin, D. W., Greenberg, P. S., and Roma, J., *Combust. Flame* 102:216–218 (1995).
3. Ku, J. C., Tong, L., Sun, J., Greenberg, P. S., and Griffin, D. W., *NASA Conference Publication 10113* (1993).
4. Ku, J. C., Tong, L., and Greenberg, P. S., *NASA Conference Publication 10174* (1995).
5. Koylu, U. O., and Faeth, G. M., *ASME J. Heat Transfer* 115:409–417 (1993).
6. Dobbins, R. A., and Megaridis, C. M., *Appl. Opt.* 30:4747–4754 (1991).
7. Ku, J. C., and Shim, K.-H., *ASME J. Heat Transfer* 113:953–958 (1991).
8. Greenberg, P. S., and Ku, J. C., submitted to *Applied Optics* (1996).
9. Ramachandran, G. N., and Lakshminarayanan, A. V., *Proc. Nat. Acad. Sci. USA*, 68:2236–2240 (1971).
10. Gulder, O. L., and Snelling, D. R., *Combust. Flame* 92:115–124 (1993).